

Cite this: *J. Mater. Chem. C*, 2020, **8**, 14880

Dielectric resonator antennas based on high quality factor MgAl₂O₄ transparent dielectric ceramics

Chao Du,^{†a} Huan-Huan Guo,^{†a} Di Zhou,^{†b} He-Tuo Chen,^{*bc} Jian Zhang,^{bc} Wen-Feng Liu,^d Jin-Zhan Su^{†e} and Hai-Wen Liu^f

For the first time, a MgAl₂O₄ transparent ceramic cylindrical dielectric resonator antenna (DRA) is designed using the fundamental HE_{11,6} modes for slot excitation. The transparent microwave dielectric ceramic was synthesized using high-purity MgO and γ -Al₂O₃ powders by aqueous gel-casting combined with cold isostatic pressing, pressure-less sintering and hot isostatic pressing methods. Optimum relative permittivity ~ 8.2 , $Q \times f$ (Q = quality factor = $1/\text{dielectric loss}$, f = resonant frequency) $\sim 110\,510$ GHz and temperature coefficient of resonant frequency ~ -74.1 ppm °C⁻¹ were obtained. The reflection coefficient, the input impedance, the antenna gain and the radiation pattern of the transparent cylindrical ceramic DRA were examined, and it was observed that the simulation results were in reasonable agreement with the measurement results. It has been found that the proposed transparent cylindrical MgAl₂O₄ ceramic DRA can provide a higher impedance bandwidth (BW = 735 MHz) and radiation efficiency (95.8%) than a state-of-the-art transparent glass DRA. The proposed configuration can potentially be used for such useful antenna decoration and can be used as a lampshade to integrate these antennas in street and traffic lights without compromising the aesthetics of the city.

Received 7th June 2020,
Accepted 22nd September 2020

DOI: 10.1039/d0tc02713h

rsc.li/materials-c

Introduction

In 1983, Long *et al.* for the first time proposed that a dielectric resonator (DR) can be used as an effective radiator,¹ which is now commonly referred to as a DR antenna (DRA). In the past three decades, the DRA has been shown to have attractive features such as small size, light weight, low loss and easy excitation,^{2,3} and the shape of the DRA can be rectangular, cylindrical, or hemispherical. By using a transparent DR,^{4,5}

however, the functions of the antenna can be diversified. This is very necessary for today's lifestyles. Now people not only pay attention to the performance of the antenna, but also pay attention to its beauty and versatility as a decorative technique.⁶

Transparent materials such as house windows, car wind-screens, kitchen containers and decorations are widely used in our daily lives today. At the same time, crystal and glassware are widely used in home and office decorations. Transparent materials with low dielectric losses can also be used as DRAs.⁷ Due to their high transparency,⁸ they can be installed on solar modules to increase the output voltage and current of solar modules without blocking sunlight.⁴ Glass DRAs can also be used as lampshades to integrate these antennas into street and traffic lights without affecting the appearance of the city. In addition, beautiful crystal art and glassware can be used as decorative antennas.⁶ If no separate or visible antenna is required, a decorative antenna can be used. However, the refractive index of glass is usually less than 1.5. This value is relatively low for DRA applications, especially when good polarization purity is required.⁶ The dispersion effect of glass is more serious in the microwave frequency band,^{9,10} which can bring some problems to the design of DRAs. Compared with glasses, transparent ceramics with a range of relative permittivity values (5–300) keep the DR's small size, light weight, low

^a Electronic Materials Research Laboratory, Key Laboratory of the Ministry of Education & International Center for Dielectric Research, School of Electronic Science and Engineering, Xi'an Jiaotong University, Xi'an, 710049, China. E-mail: zhoudi1220@gmail.com

^b State Key Laboratory of High Performance Ceramics and Superfine Microstructure, Shanghai Institute of Ceramics, Chinese Academy of Sciences, Shanghai, 200050, China. E-mail: chenhetuo@mail.sic.ac.cn

^c CAS Key Laboratory of Transparent Opto-Functional Inorganic Materials, Shanghai Institute of Ceramics, Chinese Academy of Sciences, Shanghai, 201899, China

^d State Key Laboratory of Electrical Insulation and Power Equipment, Xi'an Jiaotong University, Xi'an, China

^e International Research Centre for Renewable Energy, State Key Laboratory of Multiphase Flow in Power Engineering, Xi'an Jiaotong University, Xi'an, China

^f School of Electronic and Information Engineering, Xi'an Jiaotong University, Xi'an 710049, China

[†] Chao Du and Huan-Huan Guo contributed equally to this work.

loss and ease of excitation.^{11,12} Furthermore, transparent ceramics have low manufacturing costs and are easy to mass-produce. They can be made into large-sized and complex-shaped products. Therefore, transparent ceramics have unparalleled advantages for multi-purpose DRAs and decorative DRAs.

Magnesium aluminate spinel (MgAl_2O_4) transparent ceramics have many excellent properties, such as low density, high hardness, corrosion resistance, high strength, transparency from near-ultraviolet to mid-infrared, and high temperature stability.^{13,14} So far, various MgAl_2O_4 transparent ceramic manufacturing methods have been developed, such as pressure-less sintering (PS)/hot isostatic pressing (HIP),^{15,16} hot pressing (HP),^{17,18} spark plasma sintering^{19,20} and reaction sintering.^{21,22} Although transparent ceramics have been produced by various methods, almost all commercial production uses HP/HIP or PS/HIP.²³ Therefore, the manufacturing process of transparent ceramics is currently very mature. Up to now, MgAl_2O_4 transparent ceramics have been considered as candidates for challenging military applications, such as transparent armor, laser igniters, infrared transparent windows for missile launchers and reconnaissance pods, and transparent domes for infrared seeking missiles and ballistic protection.^{24–26} However, if MgAl_2O_4 transparent ceramics with such excellent performance can be applied to a decorative antenna or a transparent multifunctional antenna, it will make DRA resonator material more abundant and with more of a choice.

In this paper, MgAl_2O_4 spinel transparent ceramics were fabricated by HIP of sintered materials composed of fine grains. Then, a transparent ceramic cylindrical DRA using the $\text{HE}_{11\delta}$ fundamental modes for slot excitation is presented for the first time. We have proved that high-dielectric-constant transparent microwave ceramics can also be excited as transparent DRAs. In the present study, commercial CST Microwave Studio 2019[®] simulation software was used to simulate the reflection coefficient, radiation pattern, and gain of the antenna, with the results verified with measurements. Adequate consistency between the simulation results and the measurement results was achieved.

Experimental

The raw materials used in the production of transparent ceramics in this experiment were high-purity MgO powder (purity > 99.99%, Konoshima Chemical Co. Ltd, Japan) and $\gamma\text{-Al}_2\text{O}_3$ powder (purity > 99.99%, Dalian Hiland Photoelectric Material Co. Ltd, China). Using ethanol as solvent, the powder mixture of MgO and $\gamma\text{-Al}_2\text{O}_3$ was ball-milled with an $\text{Al}_2\text{O}_3/\text{MgO}$ ratio of 1.3 : 1 for 12 h. The mixture was then dried at 60 °C, and then the completely dried powder was sieved with an 80-mesh screen. To remove residual ethanol, the sieved powder was calcined at 800 °C for 6 h. The green body was pressed dry at 20 MPa and then cold isostatic pressed at 200 MPa. First, the green body was pre-sintered in air at 1500 °C for 3 h. In order to obtain transparent samples, HIP treatment was then carried out in argon at a pressure of 200 MPa at 1550 °C for 3 h. After

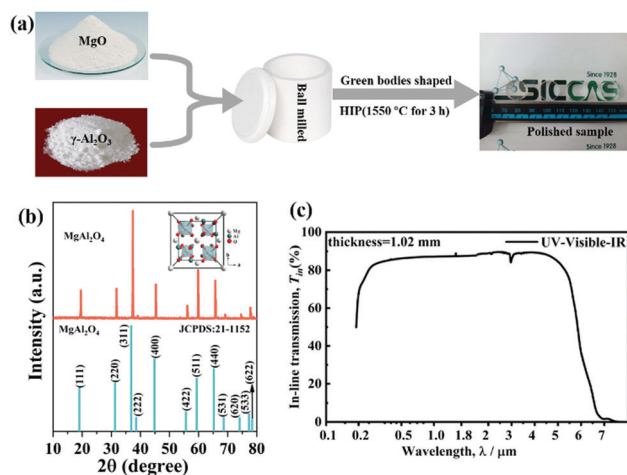


Fig. 1 (a) Schematic diagram of the experimental processes of the MgAl_2O_4 transparent microwave dielectric ceramics. (b) XRD patterns of the microwave dielectric ceramics sintered at 1550 °C (the inset is a schematic diagram of crystal structure of MgAl_2O_4). (c) In-line transmittance MgAl_2O_4 transparent ceramics at UV, visible and IR wavelengths.

6 h of air tempering at 1200 °C, the samples were processed on both sides and optically polished. A schematic diagram of the experimental processes is shown in Fig. 1(a).

X-Ray diffraction (XRD) was conducted with $\text{Cu-K}\alpha$ radiation (Bruker D2 Phaser), at 2θ between 5 and 65° in a step size of 0.02°. Dielectric properties at microwave frequency were measured with the $\text{TE}_{01\delta}$ dielectric resonator method²⁷ using a network analyzer (HP8720ES, Agilent) and a self-made heating system. The formula for calculating the temperature coefficient of the resonance frequency $\text{TCF}(\tau_f)$ was as follows:

$$\text{TCF}(\tau_f) = \frac{f_{85} - f_{25}}{f_{25} \times (85 - 25)} \times 10^6 \quad (1)$$

where f_{25} and f_{85} are the $\text{TE}_{01\delta}$ resonant frequencies at 25 °C and 85 °C, respectively.

Antenna design and optimization were carried out by using commercial simulation software CST Microwave Studio 2019[®] and the same network analyzer was used to measure the reflection parameter S_{11} of the antenna. A radiation pattern defines the variation of the power radiated by an antenna as a function of the direction away from the antenna, and the radiation patterns of the E - and H -planes were obtained by the rotating antenna method in a microwave anechoic chamber. Gain testing was done to compare the gain of the antenna under test with a standard antenna of known gain.

Results and discussion

Fig. 1(b) shows XRD patterns of MgAl_2O_4 transparent ceramics sintered at 1550 °C using MgO and $\gamma\text{-Al}_2\text{O}_3$ as raw and processed materials. All the peaks were indexed to the spinel phase (JCPDS: 21-1152) indicating there are no secondary phases. The microwave dielectric properties of MgAl_2O_4 transparent ceramics are listed in Table 1. The bulk density of the transparent ceramics, which were sintered at 1550 °C, is 3.57 g cm^{-3} , the

Table 1 Microwave dielectric properties of MgAl₂O₄ transparent ceramics and other dielectric ceramics with similar dielectric properties

Sample	T_s (°C)	ϵ_r	$Q \times f$ (GHz)	$\tan \delta$	TCF (ppm °C ⁻¹)	Ref.
MgAl ₂ O ₄	1550	8.2	110 510	7.8×10^{-5}	-74.1	This work
Ca ₃ Si ₂ O ₇	1300	7.8	28 400	2.7×10^{-4}	N/A	28
SrWO ₄	1150	7.9	56 000	1.8×10^{-4}	-55	29
CaSiO ₃	1300	8.4	16 000	5.3×10^{-4}	N/A	28
ZnAl ₂ O ₄	1375	8.5	56 000	2.1×10^{-4}	-79	30

relative density is $\sim 99.9\%$ with $\epsilon_r \sim 8.2$, $Q \times f \sim 110\,510$ GHz, and TCF ~ -74.1 ppm °C⁻¹, which are excellent among the dielectric ceramics with similar dielectric properties as shown in Table 1. Meanwhile, the dielectric loss ($\tan \delta = 0.000078$) of the sample was obtained by the closed-cavity resonance method. This method is a commonly used one to determine the dielectric constant and loss tangent of microwave dielectric materials. The cavity resonance structure is shown in Fig. 2(a). This test system generally uses the Rayleigh–Ritz method²⁷ to obtain the dielectric constant of the dielectric sample and the resonance frequency of the TE_{01 δ} mode, and then calculates the dielectric constant ($\epsilon_r = 8.2$) and dielectric loss ($\tan \delta = 0.000078$) of MAO cylindrical ceramics through parameter calculations. The MgAl₂O₄ transparent ceramics have consistently high transmittance from ultraviolet to mid-infrared. It can be seen from the transmittance curve of a 1.02 mm thick MgAl₂O₄ sample (Fig. 1(c)) that it is transparent in the wavelength range of 0.2–6.5 μm , and the transmittance can reach 83% between 0.4 and 5 μm . Meanwhile, MgAl₂O₄ transparent ceramics have excellent mechanical properties and chemical stability, and can adapt to harsh natural environments.

Based on MgAl₂O₄ transparent ceramics, we proposed a cylindrical DRA as shown in Fig. 2(b). It consists of a transparent ceramic disc DR and a microstrip slot feed structure, both of which are on the same side of the substrate. The DR ($\epsilon_{r,\text{DR}} = 8.20$; $\tan \delta = 0.000078$) has a diameter D , height h , and the bottom is stacked tightly on the slot which is etched on the center of a grounded Rogers RT5880 substrate ($\epsilon_{r,\text{sub}} = 2.20$; $\tan \delta = 0.0009$) of thickness g . A RT/duroid[®] 5880 high frequency laminate was purchased and processed in Taizhou Aoling Electronic Technology Co. Ltd. The length of the slot is w_s , the width is l_s and the width of the microstrip line coupled to it is w_f . P is defined as the side length of the

Table 2 Design parameters of the cylindrical DRA

Parameter name	Parameter	Value (mm)
DR diameter	D	15.96
DR height	h	4.36
Substrate thickness	g	1.524
Substrate length	P	50.0
Slot width	w_s	3.8
Slot length	l_s	7.9
Microstrip feed width	w_f	4.3
GP side length	s	4.2

substrate and s is the short length of the microstrip line outside the slot. With the above arrangement, it is expected that the DR resonating at the fundamental mode HE_{11 δ} has broadside radiation patterns and the slot excited DRA serves as a radiator, which can have a mode similar to HE_{11 δ} . With the assistance of the commercial CST Microwave Studio 2019[®] simulation software, the design parameters of the proposed antenna were obtained as presented in Table 2.

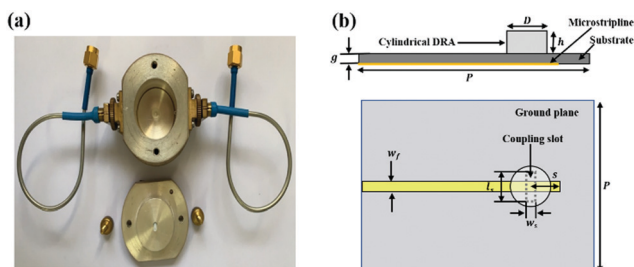
We conducted a theoretical analysis for the proposed DRA design structure. The cylindrical DRA is fed by a microstrip-coupled slot, exciting in its HE_{11 δ} mode which radiates like a short horizontal magnetic dipole.³¹ For cylindrical DRAs, the resonance frequency of their HE_{11 δ} mode can be calculated using the following technical formula:³²

$$f_{\text{HE}_{11\delta}} = \frac{6.324c}{\pi D \sqrt{\epsilon_r + 2}} \times \left[0.27 + 0.36 \times \frac{D}{4h} + 0.02 \times \left(\frac{D}{4h} \right)^2 \right] \quad (2)$$

where c is the speed of light and ϵ_r is the dielectric constant of MgAl₂O₄.

It was simulated that the cylindrical MgAl₂O₄ transparent ceramic DRA resonates at 6.7 GHz. First, the internal E - and H -fields of the resonance mode (6.7 GHz) were examined, and it was found that the field distribution is similar to the HE_{11 δ} mode.³³ The radiation of this mode has an “O” shaped far field pattern on the yo z and xoy planes like an equivalent magnetic dipole in the x -direction. With the diffraction effect of a ground plane, it radiates broadside radiation patterns. Fig. 3 shows the internal E - and H -fields of the HE_{11 δ} mode at 6.7 GHz. With reference to the figure, there is a semi-circular electric field within the DRA (yo z-plane), while the H -field is concentrated in the middle (xoz -plane). By observing the electric field and the direction of the electric field on top of the DRA (direction of the z -axis), we can also clearly see in Fig. 3(a) and (b) that the H -field is along the x -axis direction and the E -field is along the minus y -axis direction. The figure illustrates that the cylindrical MgAl₂O₄ transparent ceramic DR HE_{11 δ} mode is excited.

A prototype was made based on the optimized design using CST and photos of it are shown in Fig. 4(d) and (e). The reflection coefficient was measured with a network analyzer. Fig. 4(a) shows the antenna measurement setup and Fig. 4(c) shows a prototype of the cylindrical MgAl₂O₄ transparent ceramic DR. Fig. 4(b) shows the measured and simulated reflection coefficients of the cylindrical transparent DRA. With reference to the figure, the cylindrical transparent DRA resonates at 6.8 GHz. The measured impedance bandwidth of the

**Fig. 2** (a) A prototype of the closed-cavity resonance structure. (b) Configuration of the cylindrical DRA: side view and bottom view.

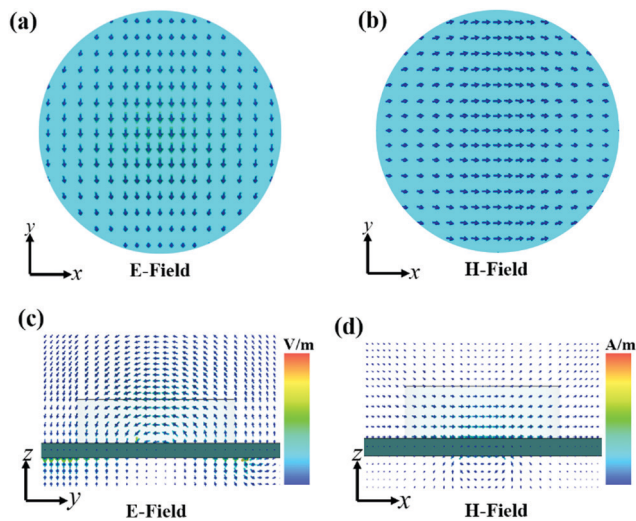


Fig. 3 Distribution of electric fields at 6.73 GHz: (a) xy -plane, (c) yz -plane. Distribution of magnetic fields at 6.73 GHz: (b) xy -plane, (d) xz -plane.

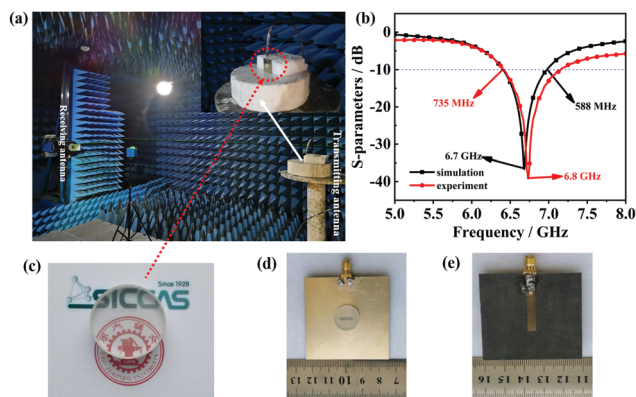


Fig. 4 (a) Antenna measuring devices. Inset shows the proposed DRA prototype. (b) Simulated (black curve) and measured (red curve) reflection coefficient of the transparent cylindrical DRA. (c) MgAl_2O_4 transparent ceramic DR. A prototype of the proposed cylindrical DRA: (d) a top view and (e) a bottom view.

cylindrical transparent DRA is 10.84% (735 MHz) agreeing very well with the simulated value of 8.78% (588 MHz), both being lower than the theoretical calculation value (14.06%). Since the preparation of MgAl_2O_4 transparent ceramics is a relatively easy process,³⁴ by making smaller or larger cylindrical MgAl_2O_4 transparent ceramic DRAs, the frequency band can be converted into a useful frequency band.

Fig. 5 shows the measured and simulated radiation patterns of a cylindrical transparent DRA, typical broadside radiation patterns being observed on two principal planes, *i.e.*, XZ -plane (H -plane) and YZ -plane (E -plane), at 6.73 GHz (simulation) and 6.8 GHz (measurement), respectively. These radiation patterns were experimentally measured in a microwave anechoic chamber. Both simulated and measured results are in good agreement. This result can be expected if the DRA is centrally fed by a coupling slot. For the E - and H -plane patterns, the co-polarized fields are stronger than the cross-polarized fields by more than 20 dB in the boresight direction ($\theta = 0^\circ$).³⁵

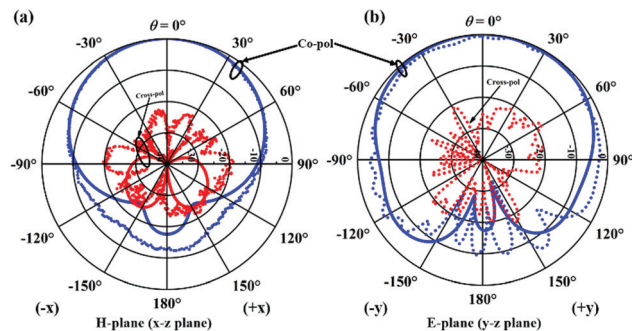


Fig. 5 Simulated and measured normalized radiation patterns of the prototype: (a) xz plane, (b) yz plane. Solid line: simulated (6.73 GHz); dotted line: measured (6.8 GHz).

Fig. 6 shows the measured and simulated antenna gains of the cylindrical MgAl_2O_4 transparent ceramic DRA at $\theta = 0^\circ$, $\varphi = 0^\circ$. Comparing the measured antenna realized gain with the simulated antenna gain, they remain consistent. Fig. 6 shows that the measured gain varies between 4.21 and 5.39 dB. The change in realized gain of the simulation result is between 4.24 and 5.45 dB, which is slightly larger than the measured value. Also, these gains are also much higher than those of slot antennas. These experimental results confirm that the resonance is caused by the ceramic DRA and not by the feed slots. Meanwhile, the simulated radiation efficiency of the entire frequency band is higher than 95.8%. This efficiency is somewhat higher than that of a conventional DRA,³⁶ which is mainly due to the low dielectric loss of the MgAl_2O_4 transparent ceramics.

Finally, it should be mentioned that transparent microwave ceramic DRAs are not only attractive for multifunctional decorative antennas, but are now becoming more attractive with the rapid development of wireless 5G communication systems. We compared the DR materials of different DRAs. From Table 3, we can find that most of the currently reported transparent DRA materials are generally glass. The loss and dispersion effect of glass is more serious in the microwave

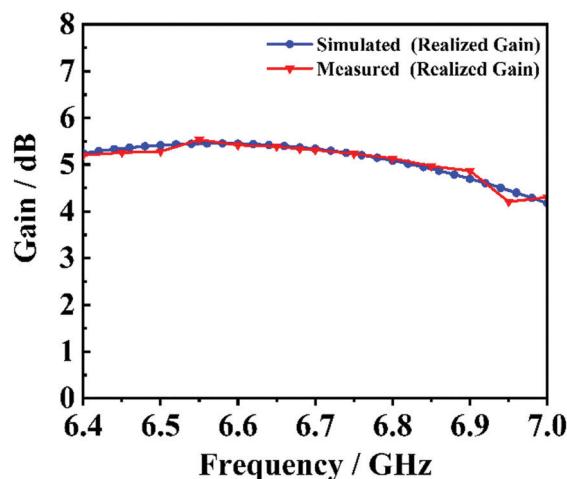


Fig. 6 Measured and simulated realized gain of the cylindrical DRA.

Table 3 Performance comparison of different DR materials

Material	Loss	Dispersion	Transparency	Ref.
MgAl ₂ O ₄ ceramics	Low	Low	High	This work
Pyrex	High	High	High	4
Pyrex	High	High	High	9
Glass	High	High	Low	37
Glass/zirconia	High	High	Low	38

frequency band,^{9,10} which can bring some problems to the design of DRAs. However, most microwave dielectric materials are oxide ceramics in which ions or atoms are linked by ionic bonds or covalent bonds. In the microwave frequency band (300 MHz–300 GHz), various slow polarization mechanisms are withdrawn from the response, and only ion polarization and electronic polarization continue to play a major role. Since the contribution of the dielectric constant in the optical frequency band produced by the electronic polarization to ϵ_r is very small and can be ignored, the ion displacement polarization determines the dielectric constant of the material in the microwave frequency band. In the ion crystal, the angular frequency of the transverse optical mode (ω_T) is 10^{12} – 10^{13} , so $\omega_T^2 \gg \omega^2$ in the general microwave range. Therefore, in the microwave frequency band, the dielectric constant of microwave dielectric materials does not change with frequency.

And the MgAl₂O₄ transparent ceramics have consistently high transmittance from ultraviolet to mid-infrared, optimum dielectric loss $\sim 7.8 \times 10^{-5}$, $Q \times f$ (Q = quality factor = 1/dielectric loss, f = resonant frequency) $\sim 110\,510$ GHz and the dielectric constant of MgAl₂O₄ transparent ceramics does not change with frequency. Meanwhile, MgAl₂O₄ transparent ceramics have excellent mechanical properties and chemical stability, and can adapt to harsh natural environments. Due to the unique advantages, printed circuit boards using microwave ceramics have the lowest high-frequency dielectric loss currently and in the foreseeable future, and will inevitably become valuable for 5G handheld devices.

Conclusions

In this study, MgAl₂O₄ transparent ceramic has been fabricated by gel-casting, isostatic pressing and PS followed by HIP. The ceramic sintered at 1550 °C exhibits excellent microwave dielectric properties of $\epsilon_r \sim 8.2$, $Q \times f \sim 110\,510$ GHz, and TCF of -74.1 ppm °C⁻¹. Meanwhile, the MgAl₂O₄ transparent ceramic fabricated by this method had excellent optical properties, making it a promising material for cylindrical MgAl₂O₄ transparent ceramic DRA application for the first time. The DRA was excited in its fundamental broadside HE_{11δ} mode using slot excitation. The commercial simulation software CST Microwave Studio 2019[®] was used to simulate the configuration and an adequate consistency was obtained between the measurement results and the simulation results. The designed cylindrical transparent DRA resonates at 6.8 GHz with a bandwidth of approximately 735 MHz ($S_{11} < -10$ dB). These results indicate that the cylindrical MgAl₂O₄ transparent ceramic DRA

has very good antenna performance. With the rapid growth in research on DRAs, it is foreseeable that more interesting and useful DRA designs will be investigated and described in the future.

Conflicts of interest

There are no conflicts to declare.

Acknowledgements

This work was supported by the National Key Research and Development Program of China (grant 2017YFB0406301), the State Key Laboratory of Electrical Insulation and Power Equipment (grant EPE19210), the Fundamental Research Funds for the Central University, and the Natural Science Foundation of Shanghai (grant no. 19ZR1465000).

Notes and references

- 1 S. A. Long, M. W. Mcallister and L. C. Shen, *IEEE Trans. Antennas Propag.*, 1983, **31**, 406–412.
- 2 H. K. Ng and K. W. Leung, *Dielectric Resonator Antennas*, John Wiley & Sons, Inc., 2005.
- 3 A. Petosa, *Dielectric Resonator Antenna Handbook*, Artech House Publish, 2007.
- 4 E. H. Lim and K. W. Leung, *IEEE Trans. Antennas Propag.*, 2010, **58**, 1054–1059.
- 5 X. S. Fang and K. W. Leung, *IEEE Trans. Antennas Propag.*, 2014, **62**, 5353–5357.
- 6 L. Kwok Wa, L. Eng Hock and F. Xiao Sheng, *Proc. IEEE*, 2012, **100**, 2181–2193.
- 7 M. S. Wu and K. Ito, *IEEE Antennas & Propagation Society International Symposium*, 1992.
- 8 J. Hautcoeur, F. Colombel, X. Castel, M. Himdi and E. Motta Cruz, *Electron. Lett.*, 2009, **45**, 1014–1018.
- 9 K. W. Leung, X. S. Fang, Y. M. Pan, E. H. Lim, K. M. Luk and H. P. Chan, *IEEE Trans. Antennas Propag.*, 2013, **61**, 587–597.
- 10 K. W. Leung, Y. M. Pan, X. S. Fang, E. H. Lim, K.-M. Luk and H. P. Chan, *IEEE Trans. Antennas Propag.*, 2013, **61**, 578–586.
- 11 A. Petosa and A. Ittipiboon, *IEEE Antennas Propag. Mag.*, 2010, **52**, 91–116.
- 12 Y. X. Guo and K. M. Luk, *IEEE Trans. Antennas Propag.*, 2003, **51**, 1120–1124.
- 13 D. C. Harris, *Proceedings of Spie the International Society for Optical Engineering*, 2005, pp. 1–22.
- 14 C. Gajdowski, J. Böhmeler, Y. Lorgouilloux, S. Lemonnier and A. Leriche, *J. Eur. Ceram. Soc.*, 2017, **37**, 5347–5351.
- 15 A. Rothman, S. Kalabukhov, N. Sverdlov, M. P. Dariel and N. Frage, *Int. J. Appl. Ceram. Technol.*, 2014, **11**, 146–153.
- 16 A. Krell, J. Klimke and T. Hutzler, *J. Eur. Ceram. Soc.*, 2009, **29**, 275–281.
- 17 L. Esposito, A. Piancastelli, P. Miceli and S. Martelli, *J. Eur. Ceram. Soc.*, 2015, **35**, 651–661.
- 18 L. L. Zhu, Y. J. Park, L. Gan, S. I. Go, H. N. Kim, J. M. Kim and J. W. Ko, *Mater. Lett.*, 2018, **219**, 8–11.

- 19 S. Benaissa, M. Hamidouche, M. Kolli, G. Bonnefont and G. Fantozzi, *Ceram. Int.*, 2016, **42**, 8839–8846.
- 20 K. Morita, B. N. Kim, H. Yoshida, K. Hiraga, Y. Sakka and I. Reimanis, *J. Am. Ceram. Soc.*, 2015, **98**, 378–385.
- 21 H. Dan, Z. Jian, L. Peng, L. Gui and S. Wang, *Ceram. Int.*, 2018, **10**, 11101–11108.
- 22 B. N. Kim, K. Morita, J. H. Lim, K. Hiraga and H. Yoshida, *J. Am. Ceram. Soc.*, 2010, **93**, 2158–2160.
- 23 M. Rubat du Merac, H.-J. Kleebe, M. M. Müller and I. E. Reimanis, *J. Am. Ceram. Soc.*, 2013, **96**, 3341–3365.
- 24 P. P. Zhang, P. Liu, Y. Sun, J. Wang, Z. J. Wang, S. W. Wang and J. Zhang, *J. Alloys Compd.*, 2015, **646**, 833–836.
- 25 S. S. Balabanov, R. P. Yavetskiy, A. V. Belyaev, E. M. Gavrishchuk, V. V. Drobotenko, I. I. Evdokimov, A. V. Novikova, O. V. Palashov, D. A. Permin and V. G. Pimenov, *Ceram. Int.*, 2015, **41**, 13366–13371.
- 26 A. Krell, T. Hutzler, J. Klimke and A. Potthoff, *J. Am. Ceram. Soc.*, 2010, **93**, 2656–2666.
- 27 J. Krupka, *Meas. Sci. Technol.*, 2006, **17**, R55–R70.
- 28 M. Valant and D. Suvorov, *J. Eur. Ceram. Soc.*, 2004, **24**, 1715–1719.
- 29 Y. J. Cho, J. Yoon, K. O. Young-San, S. Y. Kim, S. J. Cho, W. H. Kim, J. W. Park, H. D. Youn, J. H. Kim and B. L. Lee, *APMIS*, 2010, **118**, 782–790.
- 30 K. P. Surendran, N. Santha, P. Mohanan and M. T. Sebastian, *Eur. Phys. J. B*, 2004, **41**, 301–306.
- 31 R. K. Mongia and P. Bhartia, *Int. J. Microwave Mill.*, 1994, **4**, 230–247.
- 32 A. Iqbal, A. J. Alazemi and N. Khaddaj Mallat, *IEEE Access*, 2019, **7**, 184029–184037.
- 33 R. Chair, A. A. Kishk and K. F. Lee, *IEEE Microw. Wirel. Compon. Lett.*, 2005, **15**, 241–243.
- 34 B. M. Moshtaghioun, J. I. Peña and R. I. Merino, *J. Eur. Ceram. Soc.*, 2020, **40**, 1703–1708.
- 35 L. Zou, D. Abbott and C. Fumeaux, *IEEE Antennas Wirel. Propag. Lett.*, 2012, **11**, 515–518.
- 36 N. Yang and K. W. Leung, *IEEE Trans. Antennas Propag.*, 2020, **68**, 3248–3253.
- 37 N. Yang, K. W. Leung, K. Lu and N. Wu, *IEEE Trans. Antennas Propag.*, 2017, **65**, 839–844.
- 38 N. Yang, K. W. Leung and N. Wu, *IEEE Trans. Antennas Propag.*, 2019, **67**, 6778–6788.